

## Article

# Rare Earth Elements in Sediments from the Laptev Sea Shelf: Insight into Sources and Distribution Factors

Alexey Ruban <sup>1,\*</sup>, Oleg Dudarev <sup>2,3</sup>, Maxim Rudmin <sup>1</sup>  and Igor Semiletov <sup>1,2,3</sup>

<sup>1</sup> Division for Geology, Tomsk Polytechnic University, 634050 Tomsk, Russia; rudminma@tpu.ru (M.R.); ipsemiletov@gmail.com (I.S.)

<sup>2</sup> V.I. Il'ichev Pacific Oceanological Institute, Far Eastern Branch, Russian Academy of Sciences, 690041 Vladivostok, Russia; dudarev@poi.dvo.ru

<sup>3</sup> Laboratory of the Arctic Land Shelf Interaction, Tomsk State University, 634050 Tomsk, Russia

\* Correspondence: ruban@tpu.ru

**Abstract:** The study of rare earth elements (REEs) in marine sediments is a powerful geochemical tool for determining depositional processes and sediment provenance, as well as for understanding paleoenvironmental changes. In this context, we present REE, some major and trace elements, grain size, and mineralogy data on surface and core sediments, which were collected in different areas of the eastern Laptev Sea Shelf (LSS; Arctic Ocean). The primary objective of this paper was to assess the principal controlling factors influencing REE concentration and their vertical to lateral distribution. The total REE content ( $\Sigma$ REE) ranged from 139 ppm to 239 ppm within the studied sediment samples, predominantly consisting of silt. The normalized REE distribution patterns, based on North American Shale Composite (NASC) standard, exhibited an enrichment in light REE (LREE) when compared to heavy REE (HREE), which is similar to that in Lena River suspended particulate matter. The primary sources of REEs in the eastern LSS were both the suspended particulate matter from the Lena River and sediments originating from the coastal ice complex. The spatial distribution of REEs was primarily contingent upon the distance from sediment sources and prevailing hydrological conditions and was generally characterized by a decrease in REE concentration seaward. There was a moderate positive correlation between  $\Sigma$ REE and mean grain size in the studied surface sediment. However, this relationship was specific only for surface samples and was not found in the sediment cores, indicating that sediment grain size does not play a significant role in the REE vertical distribution. The strong positive correlation between  $\Sigma$ REE and Al, K, Ti, V, Cr, Zr, Hf, and Th suggests that REEs are hosted by not only heavy but also clay minerals. The vertical fluctuations of LREE/HREE, Eu/Eu\*, (La/Lu)<sub>N</sub> can point at variable dominance of one or another REE source for during sediment accumulation.

**Keywords:** rare earth elements; grain size; heavy minerals; sediment chemistry; sediment source; Siberian Arctic Shelf



**Citation:** Ruban, A.; Dudarev, O.; Rudmin, M.; Semiletov, I. Rare Earth Elements in Sediments from the Laptev Sea Shelf: Insight into Sources and Distribution Factors. *Quaternary* **2024**, *7*, 12. <https://doi.org/10.3390/quat7010012>

Academic Editor: Jef Vandenberghe

Received: 4 September 2023

Revised: 6 December 2023

Accepted: 17 February 2024

Published: 28 February 2024



**Copyright:** © 2024 by the authors. Licensee MDPI, Basel, Switzerland. This article is an open access article distributed under the terms and conditions of the Creative Commons Attribution (CC BY) license (<https://creativecommons.org/licenses/by/4.0/>).

## 1. Introduction

The Laptev Sea is a marginal Arctic Ocean sea bordered by the Taimyr Peninsula from the west, the New Siberian Islands from the east, and Eurasia from the south ([1] Figure 1). About 70% of the sea area is represented by a shelf with a depth of less than 100 m. Because of warming-induced loss of sea ice cover [2], sea level rise [3], and coastal permafrost degradation [4], the Laptev Sea Shelf (LSS) is an ideal nature laboratory for studying the effects of climate change on sedimentation processes in the land–sea system. One example of the feedback of modern sedimentation in the Arctic Seas on climate warming is the reduction in sedimentation rates that is associated with the coastline shift to the south and an increase in the distance to the primary sediment sources [5,6]. Terrigenous sediments deposited in the LSS mainly originate from multiple sources, including material transported by the large Siberian rivers' flow (Khatanga, Lena, Yana [7]) and coastal erosion

products [8]. The LSS, as part of the Siberian Arctic Shelf, is characterized by extreme spatial and temporal variability of factors controlling sediment distribution [9]. These factors include the discharge volume of rivers, the direction and intensity of currents, coastal erosion rate, sea ice formation, and its drift [10–15]. In addition, the suspended particulate matter supplied to the Laptev Sea by river runoff can be incorporated into the sea ice and transported to the Eurasian Arctic Ocean by the Transpolar Drift [16–18].

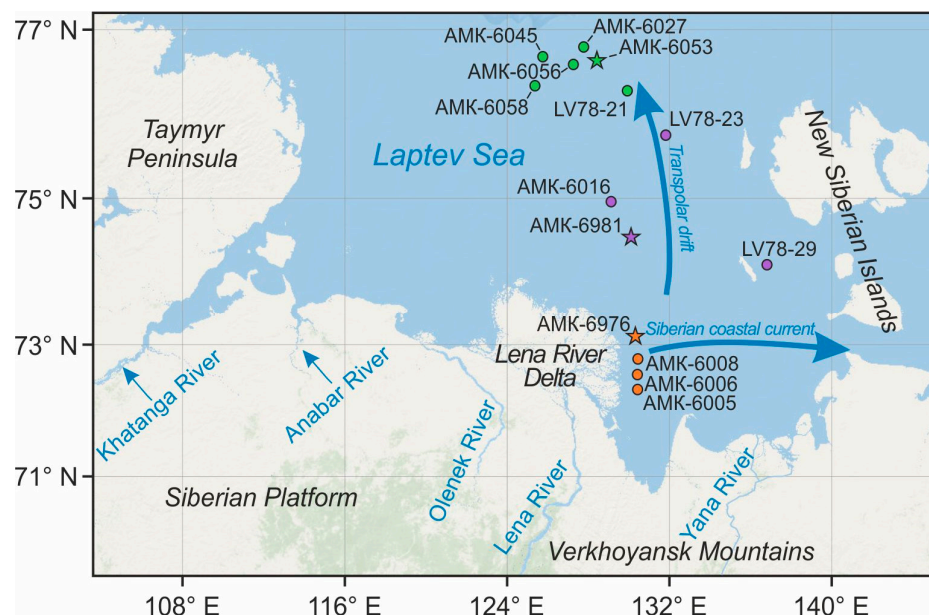


**Figure 1.** Schematic map of the study area and sampling station location (base image from ArcGIS). Circles and stars indicate the surface sediments and cores sampling locations, respectively. The symbol color indicates the confinement of sampling station to a particular shelf zone: orange—inner zone, purple—middle zone, and green—outer zone. The blue arrows show the major current features.

Rare earth elements (REEs) are the 15 elements of the lanthanide series that ranges from the lightest lanthanum (La) to the heaviest lutetium (Lu), yttrium (Y), and scandium (Sc) [19–21]. However, Sc is usually excluded because of its more similar geochemical behavior to first-row transition metals such as V, Fe, and Mn, which is caused by the much smaller ionic radius of scandium [22,23]. According to atomic weight, the lanthanide series is commonly divided into two groups: light REEs (LREE; La, Ce, Pr, Nd, Sm, Eu) and the heavy REEs (HREE; Gd, Tb, Dy, Ho, Er, Tm, Yb, Lu + Y). Since REEs are characterized by the same layout of valence electrons in outer shell, their chemical properties are similar [19,24]. The highly conservative behavior of REEs during sediment formation makes them powerful geochemical tools in the study of marine sediments for determining depositional processes and sediment provenance, as well as for understanding paleoenvironmental changes [25–30]. This is because REE content in marine sediments is primarily controlled by origin, mineralogy, and, to a lesser extent, the intensity of chemical weathering [31]. In addition, sediment grain size and biogenic material enrichment also affect the content of REEs [32,33]. However, it is important to note that some studies have shown that there is no significant influence of the grain size fractions on REE distribution [34–36].

Previous researchers have divided the Laptev Sea region into three distinct areas based on the surface sediment provenance: the eastern Laptev Sea off the Lena and Yana Rivers, the New Siberian Islands region, and the western Laptev Sea [9]. REE composition of suspended particulate material and surface sediments showed that the source of western Laptev Sea and the New Siberian Islands region sediments are sedimentary and basaltic rocks of the Siberian platform, and the source of sediments in the eastern part is fine-grained marine sedimentary rocks of the Verkhoyansk Mountains and Kolyma-Omolon super terrain [9,37]. Earlier studies of dissolved in seawater neodymium isotope and REEs

have concluded that concentrations and REE distribution patterns in the Laptev Sea are controlled by riverine inputs from the Ob, Yenisei, Khatanga, and Lena Rivers and by advection of open ocean Arctic Atlantic Water [38]. According to Sattarova et al. [39], REE distribution spectra in the sediments of the eastern Laptev Sea and particulate material of the Yana and Lena Rivers are almost identical, which also indicates a dominant role of river runoff in sediment transport.

Here, we report the REE concentrations and distribution in surface and short core (length from 14 to 30 cm) sediments collected from different part of the eastern LSS. The surface and core sediments were analyzed for the bulk contents of REEs. These measurements were combined with data on the grain size, some major and trace elements, and mineralogy in these sediment samples, from which we aimed to: (1) investigate vertical and spatial variability in REE concentration and fractionation characteristics in sediments, (2) describe the relationships between sediment features and REE distribution, and (3) constrain the factors controlling vertical and spatial distribution of REEs in the Laptev Sea sediments.

## 2. Materials and Methods

### 2.1. Study Area and Sediment Sampling

Three short cores, up to 30 cm in length, and 11 surface sediment samples (0–2 cm) were collected from the eastern LSS (Figure 1) during cruises of the research vessels “Akademik Lavrentyev” (in 2016) and “Akademik Mstislav Keldysh” (in 2018 and 2020). Core AMK-6053 (76°44′20″ N, 128°27′11″ E; water depth is 64 m) was taken from the northern part of studied area using sub-cores of a box-core sampler and penetrated 14 cm below the seafloor. Core AMK-6981 (16 cm) was collected in the eastern LSS central part with a water depth of 35 m (74°30′47″ N, 130°4′4″ E). Core AMK-6976 with a length of 30 cm was obtained in the southern part of the study area (73°6′49″ N, 130°22′2″ E; water depth is 25 m) at a distance of about 30 km from the eastern seaward boundary of the Lena River Delta. A sediment multicorer (Oktopus GmbH, Hohenwestedt, Germany) with a tube diameter of 110 mm was used for sampling cores AMK-6976 and AMK-6981. Subsampling was performed during the expedition by separating the sediment cores into slices at 1 and 2 cm intervals. The surface sediments from different area of the eastern LSS were collected using a box-corer. In total, 56 sediment samples were chosen. Every sample was divided into two parts, and all subsamples were sealed immediately in clean polyethylene bags and kept frozen until analysis. In the Tomsk Polytechnic University laboratory, half of every sample was dried to constant weight at 60 °C before further the geochemical analysis and scanning electron microscopy.

There has yet to be a generally accepted view of dividing vast LSS into separate zones. Some researchers divide the shelf of the Laptev Sea into outer and inner zones, the border between which is the 50 m isobath [40]. However, reference to the middle zone of the LSS can also be found in the literature [41]. In this paper, we identify three distinct zones in the eastern LSS. The inner zone (stations AMK-6976, AMK-6005, AMK-6006, and AMK-6008) is bounded by the Lena River Delta to the west and latitude ~74° N to the north. The middle zone (stations AMK-6981, AMK-6016, LV78-23, and LV78-29) includes the shelf part between the Lena River Delta, the New Siberian Islands, and the 50 m isobath. The outer zone (stations AMK-6027, AMK-6045, AMK-6053, AMK-6056, AMK-6058, and LV78-21) is the northern part of the eastern LSS with a water depth more than 50 m.

### 2.2. Sediment Analysis

Chemical analysis of the sediment samples was conducted at the Chemical Analytical Center “Plasma”, Tomsk, Russia. The REE contents of the sediment subsamples were determined by inductively coupled plasma mass spectrometry (ICP-MS). About 0.5 g of the each sample, ground in an agate mortar, were dissolved in ultrapure HNO<sub>3</sub>:HClO<sub>4</sub>:HF (2:2:1) and dried for 48 h under 190 °C. Then, the mixture was dissolved with 3 mL of 50% HNO<sub>3</sub> and dried at 150 °C for at least eight hours. The resulting solutions were analyzed on

an ELAN DRC-e mass spectrometer (PerkinElmer Inc., Waltham, MA, USA). The analytical precision and accuracy were better than 5% for major elements and 10% for trace elements.

Grain size analysis was performed at the Pacific Oceanological Institute (Far Eastern Branch Russian Academy of Sciences) using Analysette 22 laser diffraction particle size analyzer (Fritsch, Idar-Oberstein, Germany), with a detection range of 0.01–3800  $\mu\text{m}$ . About 2 g of sediment was suspended in deionized (DI) water using ultrasound for 5 min at the maximum pump speed. Percentages of sand, silt, and clay were derived from the distribution data using the software package GRADISTAT v.8.0 [42], which was used to calculate grain size statistical parameters. The sediments were grouped according to three-component classification [43,44] with the fractions of sand (2000–63  $\mu\text{m}$ ), silt (63–2  $\mu\text{m}$ ), and clay (<2  $\mu\text{m}$ ) fractions.

### 2.3. Scanning Electron Microscopy

REE-bearing minerals were identified by scanning electron microscopy and energy dispersive X-ray analysis (SEM-EDS). SEM-EDS were carried out on a TESCAN VEGA 3 SBU (TESCAN, Brno, Czech Republic) scanning electron microscope equipped with an OXFORD X-Max 50 (OXFORD Instruments, High Wycombe, UK) energy dispersive detector under the following parameters: a 20 kV accelerating voltage, a specimen current of 4–12 nA, and a spot diameter of approximately 0.1–2  $\mu\text{m}$ . SEM-EDS was performed at the Division for Geology, Tomsk Polytechnic University.

### 2.4. REE Parameters and Statistical Analysis

Rare earth element concentrations in sediment samples were normalized to the North American Shale Composite (NASC; [45]). Cerium ( $\text{Ce}/\text{Ce}^*$ ) and europium anomalies ( $\text{Eu}/\text{Eu}^*$ ) were calculated, respectively, as  $\text{Ce}_N/0.5 \times (\text{La}_N + \text{Pr}_N)$  and  $\text{Eu}_N/0.5 \times (\text{Sm}_N + \text{Gd}_N)$ , where N indicates NASC normalization. The LREE/HREE,  $(\text{La}/\text{Yb})_N$ ,  $(\text{Gd}/\text{Yb})_N$ , and  $(\text{La}/\text{Lu})_N$  ratios were used to quantify a fractionation between LREE and HREE. To assess the influence of seawater in the REE geochemistry of the sediments, the Y/Ho ratio was calculated. A Principal Component Analysis (PCA) was performed on geochemical and grain size data for 4 groups sediments: (i) core AMK-6976, (ii) core AMK-6981, (iii) core AMK-6053, and (iv) surface sediments. The PCA aims to identify the chemical element associations, which can explain REE distribution. The analysis was done with the STATISTICA software package for Windows (version 13.3).

## 3. Results

### 3.1. Inner Shelf

The AMK-6976 core sediments were represented by medium and coarse silt with mean grain size (Mz) ranging from 6.47  $\mu\text{m}$  to 13.07  $\mu\text{m}$  (Figure 2). The content of sand, silt, and clay in 20 studied intervals of this core varied from 0% to 7.40%, from 83.7% to 88.6%, and from 8.90% to 15.50%, respectively. The sorting coefficient ranged from 2.89 to 3.55 with an average value of 1.67, characterizing AMK-6976 core sediments as the poorly sorted. An increase in the sand entails a decrease in the clay content. The highest sand content was observed in four intervals: 0–2 cm, 4–6 cm, 10–18 cm, and 26–30 cm. In surface sediments, sand, silt, and clay varied from 0% to 0.1%, from 88.8% to 90.9%, and from 9.0% to 11.2%, respectively (Table 1).

Monazite dominated terrigenous REE minerals, occurring as relatively large grain fragments (from 2 to 40  $\mu\text{m}$ ; Figure 3c). The size of monazite differed depending on the core interval. So, the average size of monazite grains found in the interval of 5–6 cm was 19 microns, while the same in the interval of 9–10 cm was 12 microns. Among other minerals characterized by REE impurities, ilmenite, apatite, and zircon were observed.

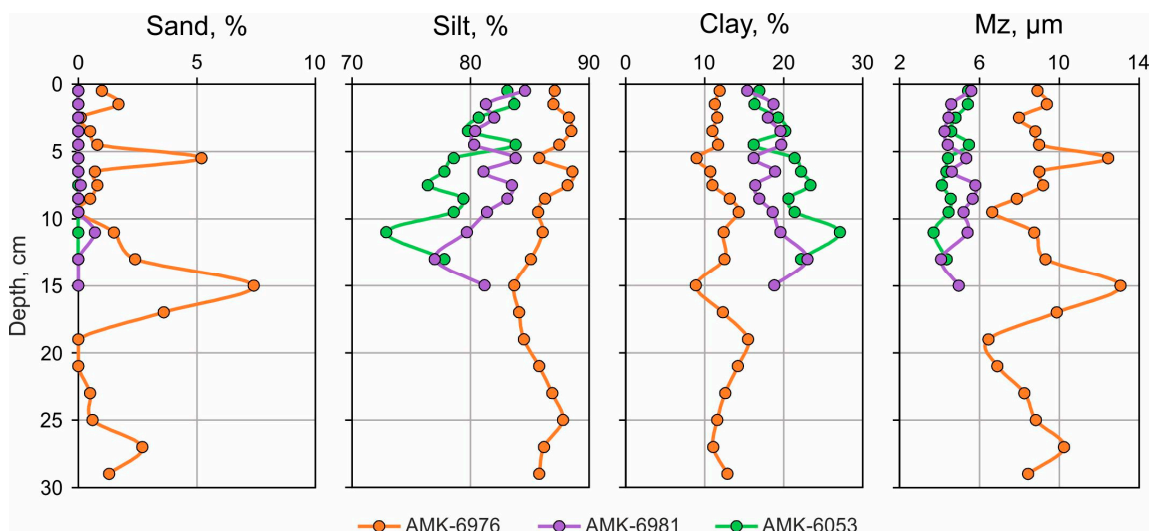


**Figure 2.** The vertical distribution of sand, silt, clay content, and mean grain size (Mz) in the studied sediment cores from the eastern Laptev Sea Shelf.

**Table 1.** Grain size data of surface sediment samples from the eastern Laptev Sea Shelf.

Samples	Water Depth, m	Sand, %	Silt, %	Clay, %	Mz, μm	Sediment Type
AMK-6005	15	0.1	90.9	9.0	10.9	Medium silt
AMK-6006	19	0.0	88.8	11.2	8.8	Medium silt
AMK-6008	22	0.0	89.1	10.9	10.1	Medium silt
AMK-6016	40	0.2	88.6	11.2	9.1	Medium silt
AMK-6027	64	0.1	89.1	10.8	7.4	Medium silt
AMK-6045	72	0.0	86.7	13.3	7.5	Medium silt
AMK-6056	62	0.0	65.2	34.8	2.9	Clayey fine silt
AMK-6058	52	0.0	83.3	16.7	5.9	Fine silt
LV78-21	56	5.3	82.1	12.6	6.1	Medium silt
LV78-23	22	0.0	83.4	16.6	6.2	Fine silt
LV78-29	20	33.7	58.4	7.9	15.6	Sandy medium silt

AMK-6976 core was characterized by the highest  $\Sigma$ REE, LREE, and HREE average relative to the other studied cores. The  $\Sigma$ REE varied slightly from 171 to 202 ppm, with an average of 189 ppm (Figure 4, Table S1). The maximum REE content was observed in the intervals of 7–10 cm and 10–14 cm, while the minimum REE content was confined to 18–22 cm and 24–26 cm. AMK-6976 core sediments were slightly enriched with  $\Sigma$ REE and LREE compared to shale composites like NASC (Figure 5). The mean of the LREE/HREE was 10.0, which is close to those of suspended particulate matter (SPM) from the Lena River (10.6) and substantially more significant than those in suspended particulate matter from the Yana River (8.1; [37]). (La/Yb)<sub>N</sub>, (La/Lu)<sub>N</sub>, (Gd/Yb)<sub>N</sub>, and Y/Ho demonstrated similar behaviors and narrow value ranges across the core. Ce/Ce\* and Eu/Eu\* exhibited a consistent vertical distribution through AMK-6976 core without a trend related to core depth. Ce/Ce\* values varied from 0.96 to 0.98 (an average of 0.97 ± 0.006), while Eu/Eu\* values ranged from 0.92 to 1.00 (average of 0.97 ± 0.02). REE concentrations ranged from 201 ppm to 211 ppm in surface sediments, while LREE/HREE values varied from 10.2 to 10.8 (Table 2). The surface sediments from inner shelf were characterized by a weak negative Eu anomaly (0.87–0.91) and no Ce anomaly.

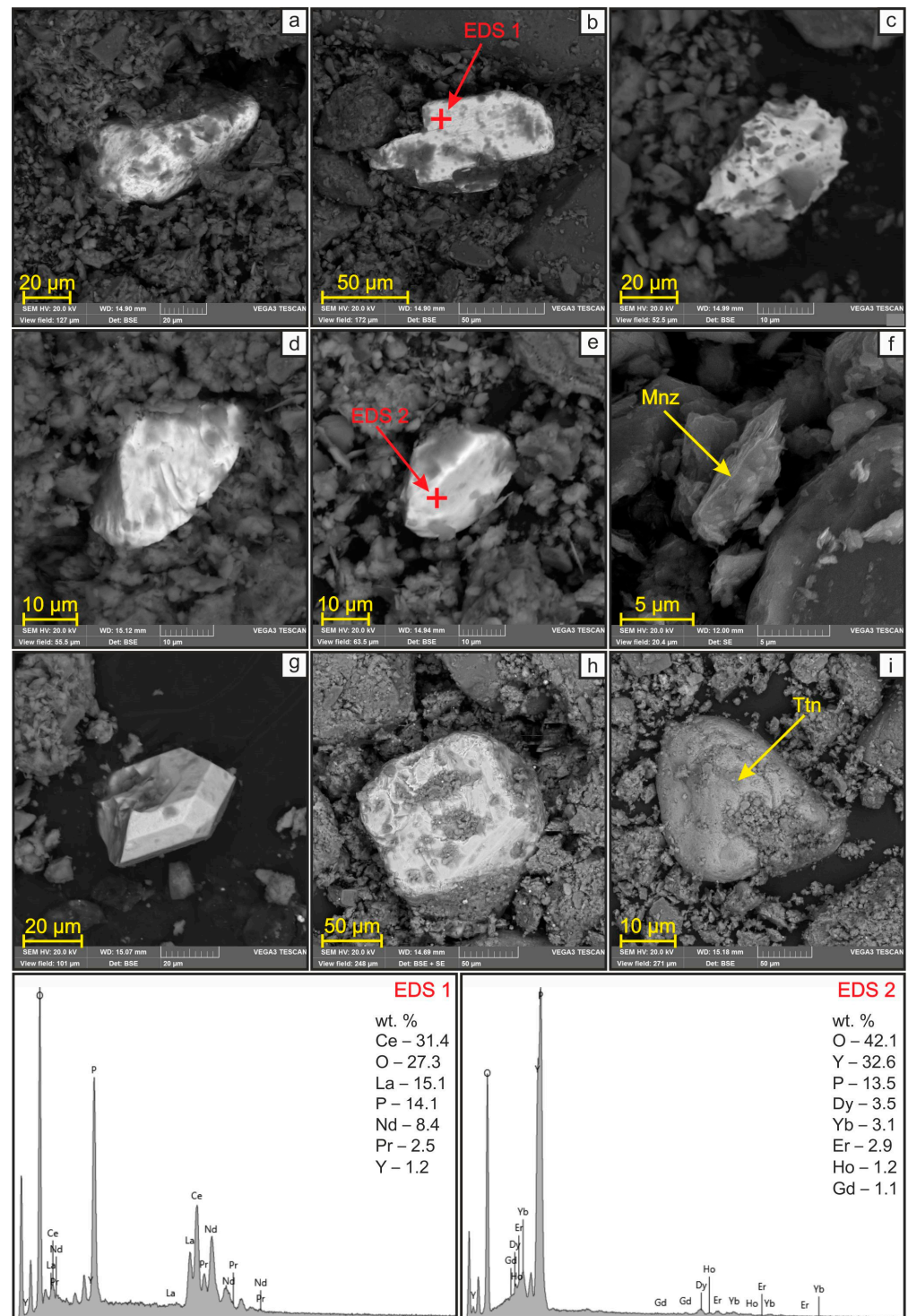


**Figure 3.** SEM images with EDS spectra of REE-bearing and other heavy minerals in the sediments from the eastern Laptev Sea Shelf: (a) monazite, AMK-6981 core (12–14 cm); (b) unrounded monazite, AMK-6981 core (8–9 cm); (c) monazite with dissolution pores (dark spots), AMK-6976 core (5–6 cm); (d) monazite, LV78-21 sample; (e) xenotime, AMK-6981 core (12–14 cm); (f) monazite, AMK-6053 core (10–12 cm); (g) unrounded euhedral zircon grain, LV78-21 sample; (h) ilmenite, AMK-6027 sample; (i) titanite, LV78-21 sample.

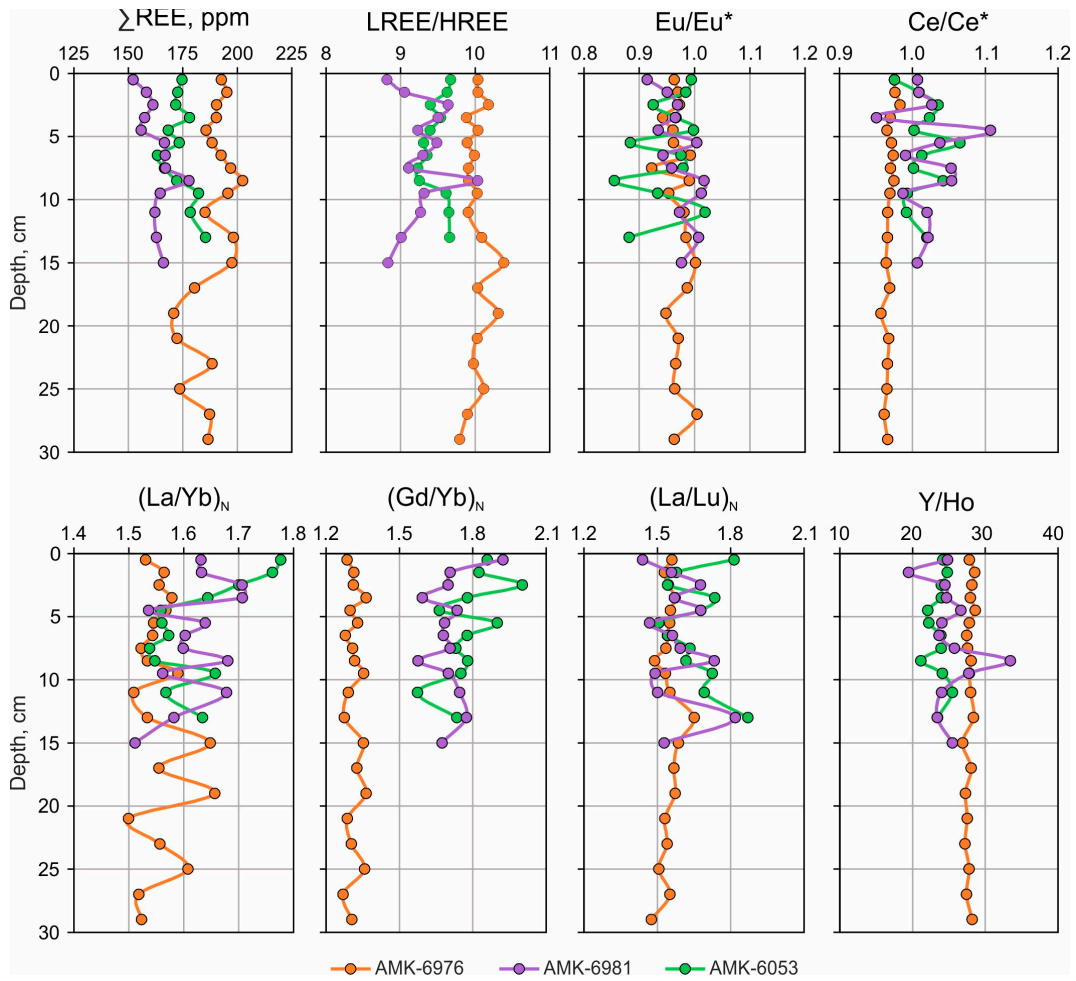


**Figure 4.** Vertical variations in REE fractionation parameters across the cores AMK-6976, AMK-6981, and AMK-6053 (additional data can be found in the Supplementary Information).

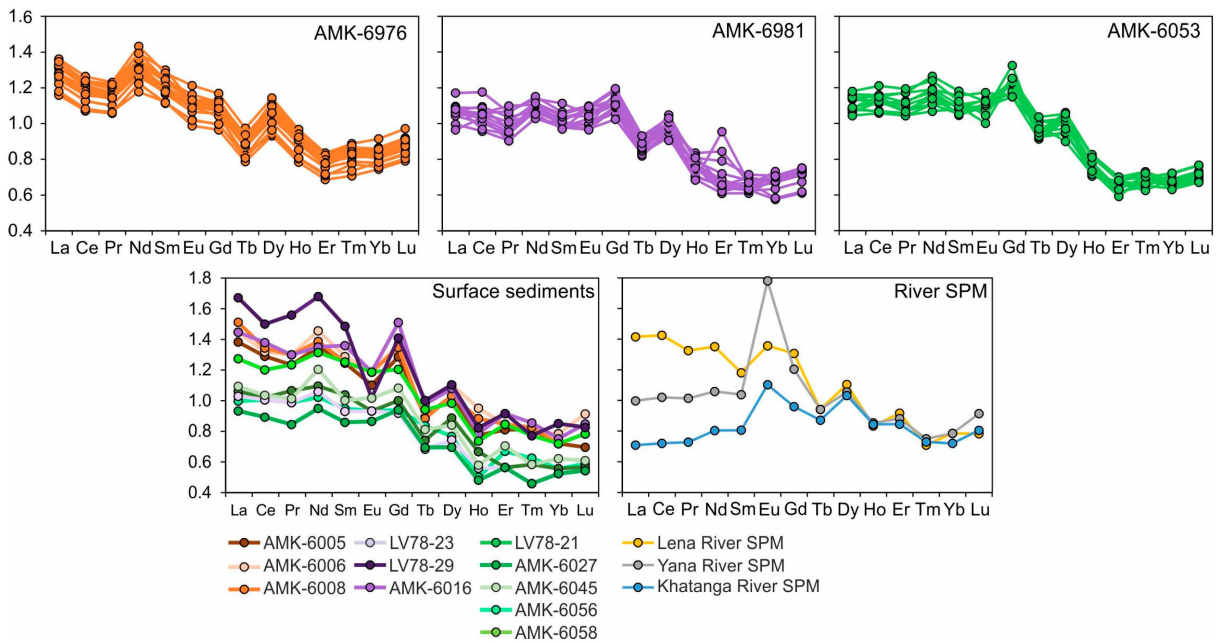


**Figure 5.** NASC-normalized REE patterns in sediment cores AMK-6976, AMK-6981, and AMK-6053, surface sediments and suspended particulate matter of the Lena, Yana, and Khatanga Rivers [37].

**Table 2.** Rare earth elements concentrations (ppm) for surface sediments from the eastern Laptev Sea Shelf.

Sample No	La	Ce	Pr	Nd	Sm	Eu	Gd	Tb	Dy	Ho	Er	Tm	Yb	Lu	ΣREE
AMK-6005	43	86	9.5	37	6.96	1.3	6.3	0.76	4.3	0.79	2.3	0.39	2.2	0.32	201
AMK-6006	45	88	10	10	7.2	1.4	6.7	0.85	4.6	0.97	2.4	0.38	2.4	0.42	210
AMK-6008	47	90	10	38	6.99	1.4	6.6	0.75	4.3	0.90	2.4	0.10	2.2	0.36	211
AMK-6016	45	92	10	37	7.6	1.4	7.4	0.83	4.5	0.80	2.6	0.41	2.3	0.39	212
AMK-6027	29	60	6.5	26	4.8	1.0	4.6	0.59	2.9	0.49	1.6	0.22	1.6	0.25	139
AMK-6045	34	69	7.8	33	5.6	1.2	5.3	0.69	3.5	0.59	2.0	0.28	1.9	0.28	165
AMK-6056	31	67	7.6	28	5.3	1.1	4.6	0.71	3.2	0.51	1.9	0.30	1.7	0.27	153
AMK-6058	40	80	9.5	36	7.0	1.4	5.9	0.8	4.1	0.75	2.4	0.37	2.2	0.36	190
LV78-21	33	68	8.2	30	5.8	1.1	4.9	0.63	3.7	0.68	1.6	0.28	1.7	0.26	160
LV78-23	32	67	7.6	29	5.2	1.1	4.5	0.58	3.1	0.57	1.6	0.22	1.6	0.25	154
LV78-29	52	100	12	46	8.3	1.2	6.9	0.85	4.6	0.84	2.6	0.37	2.6	0.38	239

A positive correlation ( $p < 0.001$ ) existed between  $\Sigma$ REE and aluminum ( $r = 0.95$ ), potassium ( $r = 0.79$ ), and titanium ( $r = 0.83$ ). In addition, a positive linear correlation between  $\Sigma$ REE and some trace elements (Cr ( $r = 0.89$ ), V ( $r = 0.87$ ), Zr ( $r = 0.81$ ), Hf ( $r = 0.83$ ), and Th ( $r = 0.90$ )) was observed. There was no correlation between REE content and grain-size parameters in AMK-6976 core sediments.

### 3.2. Middle Shelf

The middle-shelf sediments from the AMK-6981 core mainly consisted of silt (77.0–84.6%) and clay (15.4–23.0%), with an Mz average of 4.96  $\mu$ m (Figure 2), categorizing them as fine silts. The sand was observed only in two intervals (7–8 cm and 10–12 cm), with less than 0.7% content (Figure 2). The sorting coefficient, ranging from 2.37 to 3.17 (average of 2.69), characterized these sediments as poorly sorted, while the unimodal grain-size distribution suggested homogeneity of grain size. Overall, no significant change could be observed in the vertical variations in the silt and clay fractions. Except for the sample LV78-29, which was taken near the New Siberian Islands (Figure 1), the grain size of the surface sediments from the middle shelf was the same as that of the sediments in the AMK-6981 core. The sand, siltstone, and clay contents in sample LV78-29 were 33.7%, 58.4%, and 7.94%, respectively (Table 1).

The main REE-bearing minerals in the middle shelf sediments were monazite and xenotime, with grain sizes ranging from 1  $\mu$ m to 71  $\mu$ m. Only monazite, characterized by a different degree of rounding, was detected in the surface sediments, while in intervals 8–9 and 12–14 of core AMK-6981, xenotime was as common as monazite (Figure 3e).

The average  $\Sigma$ REE, LREE, and HREE concentrations in the AMK-6981 core sediments were lower than in the other two cores (Table S1).  $\Sigma$ REE varied from 152 to 178 ppm with average of 168 ppm, close to the NASC (158 ppm; [45]), and increased toward the base of the core, with maxima in the 8–9 cm interval (Figure 4). The LREE/HREE ratio of the AMK-6981 core sediments (average of 9.28) was higher than the same ratio calculated for the NASC (7.85) and was between the Lena (10.6) and Yana (8.1) Rivers' SPM (Figure 5). However, in the interval 8–9 cm, characterized by maximum REE concentration, the LREE/HREE ratio reached up to 10.0. No significant differences existed in the  $(La/Yb)_N$  ratio values (1.51–1.71 in range) among the sample within the AMK-6981. In contrast, the  $(La/Lu)_N$ ,  $(Gd/Yb)_N$ , and Y/Ho ratios were more variable, ranging from 1.44 to 1.82, from 1.58 to 1.92, and from 19.5 to 33.5, respectively. Ce/Ce\* values varied between 0.95 and 1.11 (average of  $0.97 \pm 0.04$ ) with minima and maxima in the 3–4 cm and 4–5 cm intervals, respectively. The surface sediments showed more variable REE content. So, in sample LV78-23, the REE concentration was 154 ppm, whereas in sample LV78-29, it was 239 ppm (Table 2). In addition to the maximum REE concentration, sample LV78-29 was characterized by a moderately negative Eu anomaly ( $Eu/Eu^* = 0.70$ ). The LREE/HREE and  $(La/Yb)_N$  ratios for surface sediments reached 11.5 and 1.97, respectively.

There was no linear correlation between the  $\Sigma$ REE content and the major and trace elements except Pb ( $r = 0.94$ ) in AMK-6981 core sediments. Also, no correlation between the  $\Sigma$ REE and grain-size parameters were observed in this core.

### 3.3. Outer Shelf

The sediments of core AMK-6053 were the most fine-grained of the three studied cores. The predominant grain size fraction was silt (from 72.9% to 83.8%), while clay was present in significant smaller amounts (from 16.2% to 27.1%). The sand was not detected in any of the 17 studied samples. The mean grain size ranged from 3.72  $\mu\text{m}$  to 5.49  $\mu\text{m}$  (average of 4.65  $\mu\text{m}$ ), categorizing sediments from the AMK-6053 core as fine silts (Figure 2). The values of the sorting coefficient with an average of 2.72 indicate that these sediments were also poorly sorted, while unimodal grain-size distribution suggests a homogeneity of grain size. The silt content decreased toward the base of the core and, conversely, clay content increased with depth. Sand content in surface sediments reached 5.3% (sample LV78-21), while silt and clay ranged from 65.2% to 83.3% and from 12.6% to 34.8%, respectively (Table 1).

In both surface and core sediments, monazite was the only mineral in which the content of rare earth elements has been recorded. Other heavy minerals also found include zircon, ilmenite, and titanite (Figure 3g–i). Monazite grain size in the sediment samples ranged from 1  $\mu\text{m}$  to 13  $\mu\text{m}$ , except for sample LV78-21, which contained grains with cross-sectional sizes up to 58  $\mu\text{m}$  (Figure 3d).

In AMK-6053 core, the total REE content, LREE, and HREE varied from 163 to 186 ppm (average of 157 ppm), from 15.8 to 17.4 ppm (average of 16.6 ppm), and from 148 to 168 ppm (average of 157 ppm), respectively (Figure 4; Table S1). The LREE/HREE values showed a narrow range from 9.23 to 9.67 (an average of 9.47), close to that in the studied sediments from middle shelf. The NASC-normalized REE patterns were similar throughout the AMK-6053 core (Figure 5), but vertical distributions of  $(\text{La}/\text{Yb})_{\text{N}}$  and  $(\text{Gd}/\text{Yb})_{\text{N}}$  ratios tended to decrease with depth. The Y/Ho ratio varied from 21.2 (interval of 8–9 cm) to 25.5 (interval of 10–12 cm; Figure 4). Eu/Eu\* and Ce/Ce\* averages were similar to those in the AMK-6976 and AMK-6981 cores. However, Eu/Eu\* values varied over a broader range with minima (0.85) in the 8–9 cm and maxima (1.02) in the 10–12 cm. The total REE content demonstrated a positive correlation ( $r > 0.70$ ) with some trace elements (Cr, Cu, Zr, Ba) and no correlation with grain-size fractions. The correlation coefficients ( $p < 0.001$ ) between  $\Sigma$ REE and silt content and between  $\Sigma$ REE and clay content were -0.20 and 0.20, respectively. The total REE content in the surface sediments from the outer zone of the eastern LSS varied from 139 ppm to 190 ppm (Table 2). The average value of the LREE/HREE ratio was 10.4, which is similar to that in the Lena River SPM. Eu/Eu\* values ranged from 0.92 (sample LV78-21) to 0.99 (sample AMK-6056).

## 4. Discussion

### 4.1. Rare Earth Elements Distribution and Potential Sources

It is known that concentration of the rare earth elements in continental margin sediments decreases with distance from the coastline and estuaries, which has been shown and explained by many authors in different seas, including the Arctics [9,46–48]. This is because the ratio of the land-derived sediments, which are the main carriers of REE, gradually reduces with distance from the coast. Similar REE distribution specificity is characteristic of the studied eastern LSS sediments. Due to the lack of published REE composition data for watershed rocks, we have to suggest one or another hypothetical REE source relying on river suspended particulate matter REE patterns and REE spatial distribution.

In terms of water discharge, the Lena (590 km<sup>3</sup>), Khatanga (105 km<sup>3</sup>), Yana (36 km<sup>3</sup>), and Olenyok (36 km<sup>3</sup>) are the major rivers of the Laptev Sea [49–51]. In general, the Lena, Khatanga, and Yana Rivers' SPM had the same HREE content compared to NASC, but the difference between them was the LREE content (Figure 5; [37]). So, the Lena River SPM displayed REE patterns characterized by a slight enrichment in LREE, while the Khatanga

SPM showed LREE depletion. A flat LREE distribution and a pronounced positive Eu anomaly defined the REE pattern of average Yana River SPM. The NASC-normalized REE distribution spectra in the studied surface and core sediments from the inner zone of the eastern LSS and the average value of the LREE/HREE ratio were practically identical to those for the Lena River SPM. In addition, these sediment samples were collected about 30 km from the eastern seaward boundary of the Lena River Delta. Consequently, REE composition of the inner shelf sediments studied was formed primarily under the influence of Lena River runoff. However, the Lena River drained a large catchment area (2.49 million km<sup>2</sup>) of heterogeneous geology, which is evident in REE composition of its tributaries SPM [37]. Moreover, there is no consensus on how much of this material reaches the shelf. Alabyan et al. [52] and Dudarev et al. [53] reported that only 10–17% of the sedimentary material entering the Lena River Delta reaches the Laptev Sea, while the rest is dispersed in the delta. In contrast to this statement, Rachold et al. [54] concluded that most of the Lena River's suspended sediments are supplied to the sea. Considering this, figuring out which Lena River watershed rocks are sources of REE is a challenge. The estimates of riverine sediment discharge and sediment input by coastal erosion demonstrate that the Laptev Sea coast delivers more than twice as much sediment mass as river runoff [54]. Unfortunately, in this study, we cannot consider the northern Eurasia coast ice complex erosion and the Yana River SPM's effect on sediment REE composition due to the lack of sediment samples from adjacent areas. However, we assume the Siberian coastal current can limit the role of these sediment sources in sedimentation at the middle and outer zones, because, as noted earlier, it contributes to eastward material transport [9,25,55]. According to Taylor and McLennan [56], REE composition in fine-grained sediments on continental margins is similar to the NASC and PAAS (Post Archean Australian Shale) but is characterized by HREE depletion. In general, the studied sediments from the inner shelf of the Laptev Sea were characterized by enrichment in LREE and a weak HREE depletion (except for Dy) compared to NASC. The NASC-normalized REE patterns were similar along the core AMK-6976, which indicates the same source of sediment for the entire period of sediment accumulation. Additionally, average values of Ce/Ce\* and Eu/Eu\* were close to one, indicating the lack of Ce and Eu anomalies and the same lanthanides behavior throughout the entire length of the core.

The studied sediments from the middle zone of the eastern LSS had a rather uneven REE distribution. Surface sediments from stations AMK-6981 and LV78-23 were characterized by LREE concentrations comparable to those in the NASC and reduced HREE content. AMK-6016 and LV78-29 samples were enriched in LREE, and HREE content was comparable to the NASC. Such a REE distribution pattern can be explained not only by different distances from the coastline and the Lena River Delta but also by mixing sedimentary material from several sources and the contrasting hydrological regimes. The maximum REE concentration among all studied samples was found in sample LV78-29, collected near the New Siberian Islands coast (Stolbovoy Island). This sample was characterized by a moderate negative europium anomaly ( $Eu/Eu^* = 0.70$ ), a maximum LREE/HREE ratio (11.5) greater than that of the Lena River SPM, and a maximum sand content. Apparently, sedimentary material with a different REE composition than the Lena River SPM is supplied from the New Siberian Islands (more likely from certain areas thereof) to the LSS.

The NASC-normalized REE patterns of the core AMK-6981 indicate increased (relative to core background) erbium content in some subsamples. In addition, xenotime was often observed in the core sediments of the middle shelf, whereas it was found only twice in the inner shelf sediments. Based on clay mineralogy and multi-element chemistry data, Viscosi-Shirley et al. [9] showed that the composition of New Siberian Islands region sediments and the eastern LSS sediments is different. So, low Si/Al and Mg/K ratios and high Ce concentrations indicate that shale deposits of Verkhoyansk Mountains and Kolyma-Omolon superterrain are sources for the sediments of the southeastern Laptev Sea. Sediments of the New Siberian Islands region are characterized by elevated Si/Al ratios, which correspond to sandstone sources. Obviously, the New Siberian Islands, composed by

the ice complex [57], are a significant source of sediments, entering the eastern LSS middle and outer zones. Thermal erosion promotes denudation of the ice complex and the material supply to the coastal area, from where this material can subsequently be transported westward by sea currents [58]. In the sediments of core AMK-6981, unlike cores AMK-6976 and AMK-6053, the correlation between LREE and HREE was weak (Figure 6a), which may also indicate multiple REE sources. Probably, the observed  $\Sigma$ REE, LREE/HREE, and  $(La/Lu)_N$  fluctuations in the AMK-6981 core reflect the variable dominance of one or another sediment source. In addition to river runoff and coastal ice complex erosion, sedimentary material can also be supplied by the ice rafting effect.

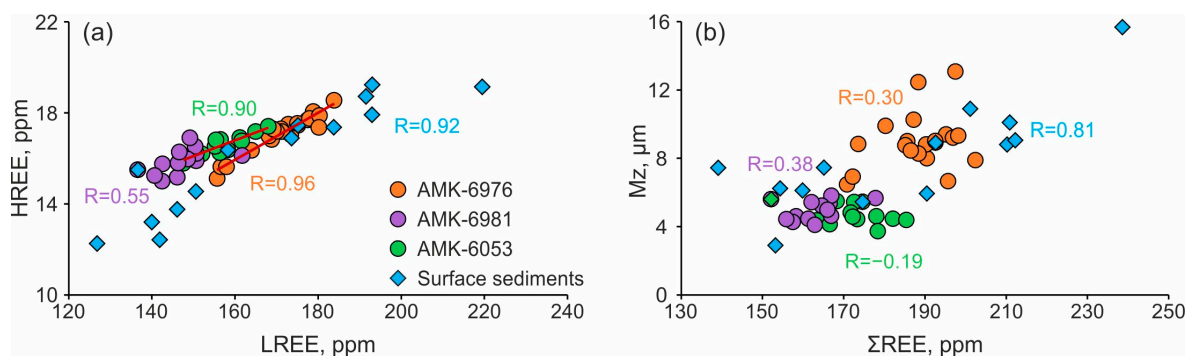


**Figure 6.** (a) A relationship between LREE and HREE. (b) Total REE concentrations as a function of mean grain size.

Despite the relatively close location of sampling stations, the REE concentrations in outer-shelf sediments ranged from 139 ppm to 190 ppm. It is known that Lena River water is transported to the north through the Transpolar Drift [59–61]. In addition to river water, the Transpolar Drift transports sea ice to seaward, including anchor ice, which can capture sediments near the coastline or in the shallows. Consequently, sea currents may transport Lena River SPM and shallow sediments to the outer shelf. However, the outer shelf of the Laptev Sea also receives sedimentary material from the western part of the Laptev Sea, the Kara Sea, and the New Siberian Islands. All studied surface sediment samples had similar  $(La/Yb)_N$ ,  $(Gd/Yb)_N$ ,  $(La/Lu)_N$ , LREE/HREE,  $Ce/Ce^*$ , and  $Eu/Eu^*$  values, which were close to those in the Lena River SPM. This fact suggests that one of the primary sources of REEs in the eastern LSS outer zone sediments is the Lena River SPM, which is transported there by the Transpolar Drift. AMK-6053 core sediments were characterized by a weak negative anomaly ( $0.85 < Eu/Eu^* < 0.9$ ) in three intervals (Figure 4). Among the studied sediment samples, a moderate negative europium anomaly was found in sample LV78-29 ( $Eu/Eu^* = 0.70$ ). Apparently, the local coastal erosion of the New Siberian Islands contributes to the sediment accumulation with a negative europium anomaly. Episodic changes in the outer shelf hydrological regime and alteration of the coastal erosion dynamic can explain the depth variability of  $Eu/Eu^*$ . It should also be taken into account that the composition of eroded ice complex can be heterogeneous, which means that the composition of the sedimentary material carried offshore is prone to change with time.

The studied surface and core sediment samples demonstrated Y/Ho ratios ranging from 19.5 to 33.5 with an average value of 26.2, which is close to that in Siberian River's SPM [37]. Such low Y/Ho value rules out significant seawater influence in REE geochemistry of the sediments [62] since seawater Y/Ho varied from 44 to 74 [63]. The maximum of the Y/Ho ratio (33.5) was confined to the 8–9 cm interval of core AMK-6981, where an increased concentration of Y (relative to the whole core AMK-6981) was observed (Table S1). It was in this interval that xenotime was most frequently encountered according to SEM.

#### 4.2. Controlling Factors of REE Distribution

Marine sediment REE properties are controlled by many factors, including grain size, mineralogical composition, marine biogenic components, diagenesis, hydrological

regime, etc. [28,48,64–66]. The grain size influence on REE content in sediments is explained by the fact that coarse sediment contains abundant REE-free quartz, while fine sediments are dominated by clay minerals, which are enriched in REEs [29,67,68]. However, grain size can affect REE distribution apparently only in terrigenous sediments of continental margins, since in authigenic marine sediments, there is no relationship between grain size and REE content, as demonstrated in phosphorites from Eastern Algeria [36].

A moderate correlation existed between  $\Sigma$ REE and Mz in the studied surface sediment, indicating an increase in REE content with increasing mean grain size (Figure 6b). However, this correspondence was only characteristic of the surface samples and was not found in any cores. For example, Mz values in the AMK-6976 core sediments varied from 6.47  $\mu$ m to 13.07  $\mu$ m, which was caused by sand concentration up to 7.4% in some intervals. However, the same REE concentrations were observed in the intervals with Mz values differing by a factor of  $\sim 2$  (Figures 2 and 4). There was no sand in cores AMK-6981 and AMK-6053 due to the large distance from the coastline and the Lena River Delta; as a result, Mz varied in a narrower range compared to the studied core from the inner shelf. Although the values of the correlation coefficient between Mz and REEs in cores AMK-6981 and AMK-6053 did not exceed 0.4 ( $p < 0.001$ ; Figure 6b), the depth profiles demonstrated a weak increase in REE concentrations from top to bottom, accompanied by a decrease in the mean grain size (Figures 2 and 4). This can indirectly indicate that the relationship between  $\Sigma$ REE and sediment grain size becomes clearer with distance from sediment provenance, since the presence of REE-bearing heavy minerals in nearshore sediments can destructed the so-called “grain size effect” [34,67]. In addition, we hypothesize that early diagenetic sediment alterations can lead to the redistribution of REEs due to dissolution REE-bearing minerals (Figure 3c).

Principal Component Analysis, which has been successfully applied to marine sediments [36,62,64,69], was performed on REE, major elements, trace elements, and some grain size parameters in order to explain the different recorded correlations (Figure 7). The main components for core AMK-6976 (inner shelf), PC1 and PC2, gathered 69.1% of the total variance (PC1 = 50.5%, PC2 = 18.6%, PC3 = 12.7%, PC4 = 7.7%). The PC1 demonstrated one distinct major trend with very high loading, which included Fe, Mg, K, Ti, Al, Zr, and Cr. The positive loading of PC1 indicates the influence of mineral composition. Obviously, positive relationships ( $p < 0.001$ ) between REEs and Ti, V, Cr, Zr, Hf, and Th (Figure 8; Table S2) were caused by the presence of REEs as an impurity in such heavy minerals as ilmenite, zircon, titanite, etc. At the same time, the correlation with Al and K can indicate that REEs were adsorbed onto or incorporated into Al and K-containing clay minerals. These findings align with the results documented by Wang et al. [48] and Yang et al. [29], showing that the lanthanides' adsorption in clay component is one of the main factors affecting their distribution. Sand and Mz had a strong positive loading toward PC2 that could reflect the “grain-size effect”. However, sediment grain size, as discussed above, does not seem to play a significant role in the REE vertical distribution in the studied inner shelf sediments. The PCA results for core AMK-6053 (outer shelf) showed that the two main components, PC1 and PC2, gathered a cumulative variance of 73.9% (PC1 = 40.4%, PC2 = 33.5%), while other components displayed less importance in term of variance (PC3 = 9.5%, PC4 = 8.2%, PC5 = 2.7%). The PC1 with the highest variance was characterized by the positive loading of Fe, Cr, Y, Zr, Ti, and clay fraction and represents heavy minerals less than 2  $\mu$ m in size. The PC2 showed strong positive loading to Al, K, and clay fraction and negative loading to Ti, Zr, Cr, silt, and Mz and may reflect the clay minerals. It is likely that REE content and vertical distribution in outer-shelf sediments was also controlled by accessory minerals. The main components for core AMK-6981 (middle shelf), PC1 (23.9%) and PC2 (18.9%), gathered 42.8% of the total variance. PC1 had positive loadings of silt fraction and Mz and negative loadings of clay and Fe. This principal component reflects the grain-size composition. PC2 was characterized by positive loading of only Mn and negative loadings of Ti, Al, Mg, and Zr. We suggest that PC2 may reflect diagenetic alterations. However, in the case of the AMK-6981 core, Principal Component Analysis, as well as Pearson's

correlation, failed to identify the factors controlling the vertical distribution of REE. This may have been caused not only by multiple sediment sources on middle shelf, but also by changing hydrological regime during the sedimentation period, as well as by early diagenetic processes. On the middle shelf, these factors may play a more significant role than on the outer shelf due to the massive mixing of river and sea waters. PCA for surface sediments showed that the first two principal components (PC1, PC2) explained 33.3% and 27.7% of the total variance, respectively, accounting for 61% of the total variance of the data set. Ti, Zr, Mn, and Al, as well as mean grain size, all had fairly high loadings on PC1, indicating that not only mineral composition but also hydrodynamic separation controls the REEs spatial distribution in surface sediments from the eastern LSS.

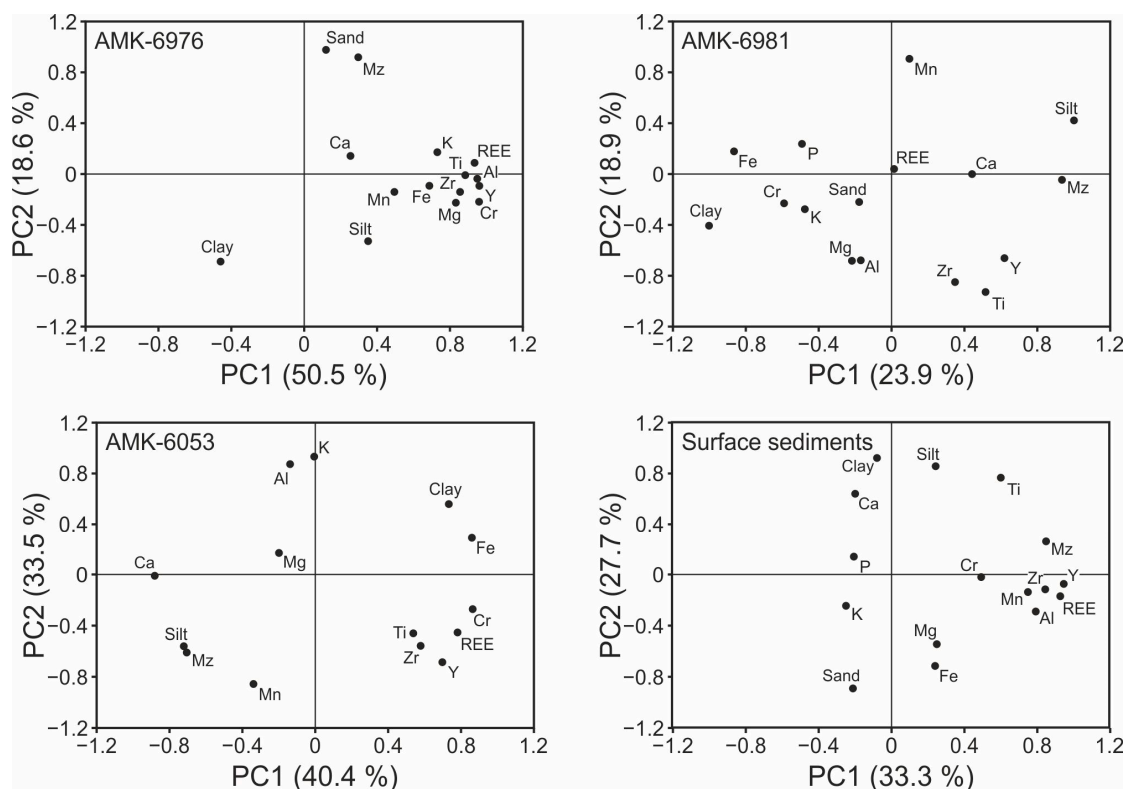


**Figure 7.** Loading the PC1 versus PC2 factors from the Principal Component Analysis (PCA) of geochemical and grain size data of studied surface and core sediments from the eastern Laptev Sea Shelf.

The individual REE concentrations in surface and AMK-6976 core sediments significantly correlated ( $r > 0.7$ ;  $p < 0.001$ ), implying that REEs were migrated and transported as an integral whole. However, in AMK-6053 core sediments, there was a strong positive correlation only between some REEs (mainly LREE). There were almost no significant correlations between individual REEs in the AMK-6981 core. This observation can also support the assumption that the eastern LSS middle- and outer-zone sediments have multiple sources, the contribution of which varied over the period of sediment accumulation.

Bau and Dulski [70] reported that the cerium anomaly values would be significant if  $Ce/Ce^* > 1.05$  or  $< 0.95$ . In our case, only 3 of the 56 studied sediment samples demonstrated such  $Ce/Ce^*$  values: sample AMK-6981 (4–5 cm), sample AMK-6053 (5–6 cm), and sample LV78-29 (Table 3 and Table S1). On the one hand, this fact can point at some vertical variability in the redox conditions of pore water in middle shelf core sediments, but on the other hand, the terrigenous material can carry the Ce anomaly pattern virtually unchanged by early diagenetic processes [71]. If the observed weak Ce variability was due to unchanged terrigenous material, this also reflects the variable dominance different material source during sediment accumulation. It is important to note that the slight Ce

anomalies could have been due to low analytical precision for La and Ce compared to other REE, using the ICP-MS method [72,73].

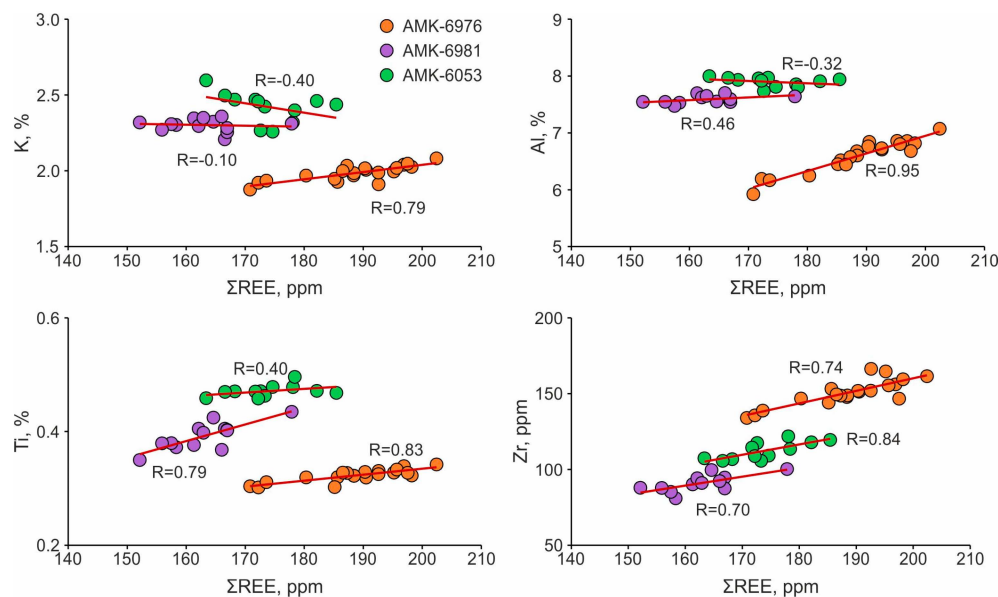


**Figure 8.** Binary cross-correlation plots of the total REE content and some major and trace elements concentrations in the studied core sediments.

**Table 3.** Fractionation parameters of rare earth elements for studied surface sediments from the eastern Laptev Sea Shelf.

Sample No	LREE/HREE	Eu/Eu*	Ce/Ce*	La/Yb	Gd/Yb	Y/Ho
AMK-6005	10.6	0.87	0.99	1.92	1.79	27.8
AMK-6006	10.2	0.89	0.96	1.84	1.74	24.7
AMK-6008	10.8	0.91	0.96	2.10	1.87	25.5
AMK-6016	10.0	0.83	1.00	1.93	1.71	26.3
AMK-6027	10.4	0.96	1.00	1.78	1.80	28.6
AMK-6045	10.4	0.98	0.98	1.76	1.74	28.8
AMK-6056	10.6	0.99	1.01	1.79	1.69	27.5
AMK-6058	10.3	0.97	0.96	1.77	1.67	26.7
LV78-21	10.6	0.92	0.96	1.91	1.80	23.5
LV78-23	11.4	1.01	1.00	1.97	1.76	28.1
LV78-29	11.5	0.70	0.93	1.97	1.66	28.6

### 5. Conclusions

REE, some major and trace elements, grain size, and mineralogy analysis of the surface and core sediments from the eastern Laptev Sea Shelf has led to the following major conclusions:

- (1) The  $\Sigma$ REE ranged from 139 ppm to 239 ppm in the studied sediment samples, mainly silt. The NASC-normalized REE distribution patterns were characterized by enriched light REEs compared to heavy REEs, which is similar to that in Lena River SPM. In general, sediments were characterized by no Ce and Eu anomalies, but nearshore and some core sediment samples demonstrated weak or moderate Eu depletions.
- (2) Heavy minerals distrust “the grain-size effect” of REE distribution, causing a positive correlation between mean grain size and the total REE content in surface sediments. A weak increase in REE concentrations, accompanied by a decrease in the mean grain size in cores from the outer shelf, can indicate a change in REE occurrence form due to diagenetic alterations. Close correlations between the  $\Sigma$ REE and Ti, V, Cr, Zr, Hf, and Th point to the presence of REEs in heavy minerals, while the strong correlation with

Al and K may indicate REEs accumulation in clay minerals. Thus, REE concentrations are primarily controlled by sediment genetic properties.

- (3) There were significantly positive correlations only between some individual REE concentrations in core sediments from the middle and outer, implying multiple REE sources. The primary REE sources for the study area were the Lena River SPM and the coast ice complex sediments. The REE composition of sediments depends on the relative contributions of these two sources. Vertical fluctuations of some geochemical indicators apparently reflect the variable dominance of one or another REE source during sediment accumulation.

**Supplementary Materials:** The following supporting information can be downloaded at: <https://www.mdpi.com/article/10.3390/quat7010012/s1>, Table S1: REE, some major and trace elements concentrations in cores AMK-6976, AMK-6981 and AMK-6053 collected from the eastern Laptev Sea Shelf; Table S2: Correlation coefficient matrix of REE, some major and trace elements, and grain size fractions for sediment core AMK-6976 from the eastern Laptev Sea Shelf.

**Author Contributions:** Conceptualization, A.R.; methodology, A.R. and M.R.; formal analysis, A.R. and M.R.; writing—original draft preparation, A.R.; writing—review and editing, A.R., O.D., M.R. and I.S. All authors have read and agreed to the published version of the manuscript.

**Funding:** This research was supported by the Russian Science Foundation (grant No. 23-77-10002). Field campaigns were supported by the assignment of the Russian Ministry of Science and Higher Education (theme 121021500057-4 to the POI FEB RAS).

**Data Availability Statement:** Data will be made available on request.

**Acknowledgments:** M.R. acknowledges Ministry of Science and Higher Education of the Russian Federation (project FSWW-2023-0010). We grateful to four anonymous reviewers whose comments helped to significantly improve this manuscript.

**Conflicts of Interest:** The authors declare no conflicts of interest.

## References

- Dobrovolsky, A.D.; Zalogin, B.S. *Morya SSSR*; Moscow State University: Moscow, Russia, 1982.
- Cai, Q.; Wang, J.; Beletsky, D.; Overland, J.; Ikeda, M.; Wan, L. Accelerated Decline of Summer Arctic Sea Ice during 1850–2017 and the Amplified Arctic Warming during the Recent Decades. *Environ. Res. Lett.* **2021**, *16*, 034015. [CrossRef]
- Ward, R.D. Sedimentary Response of Arctic Coastal Wetlands to Sea Level Rise. *Geomorphology* **2020**, *370*, 107400. [CrossRef]
- Are, F.E. The Role of Coastal Retreat for Sedimentation in the Laptev Sea. In *Land-Ocean Systems in the Siberian Arctic: Dynamics and History*; Springer: Berlin/Heidelberg, Germany, 1999; pp. 288–295. [CrossRef]
- Bauch, H.A.; Mueller-Lupp, T.; Taldenkova, E.; Spielhagen, R.F.; Kassens, H.; Grootes, P.M.; Thiede, J.; Heinemeier, J.; Petryashov, V.V. Chronology of the Holocene Transgression at the North Siberian Margin. *Glob. Planet. Chang.* **2001**, *31*, 125–139. [CrossRef]
- Rusakov, V.Y.; Borisov, A.P. Sedimentation on the Siberian Arctic Shelf as an Indicator of the Arctic Hydrological Cycle. *Anthropocene* **2023**, *41*, 100370. [CrossRef]
- Rachold, V.; Alabyan, A.; Hubberten, H.W.; Korotaev, V.N.; Zaitsev, A.A. Sediment Transport to the Laptev Sea—Hydrology and Geochemistry of the Lena River. *Polar Res.* **1996**, *15*, 183–196. [CrossRef]
- Rachold, V.; Eicken, H.; Gordeev, V.V.; Grigoriev, M.N.; Hubberten, H.-W.; Lisitzin, A.P.; Shevchenko, V.P.; Schirrmeister, L. Modern Terrigenous Organic Carbon Input to the Arctic Ocean. In *The Organic Carbon Cycle in the Arctic Ocean*; Springer: Berlin/Heidelberg, Germany, 2004; pp. 33–55. [CrossRef]
- Viscosi-Shirley, C.; Mammone, K.; Pisias, N.; Dymond, J. Clay Mineralogy and Multi-Element Chemistry of Surface Sediments on the Siberian-Arctic Shelf: Implications for Sediment Provenance and Grain Size Sorting. *Cont. Shelf Res.* **2003**, *23*, 1175–1200. [CrossRef]
- Feng, D.; Gleason, C.J.; Lin, P.; Yang, X.; Pan, M.; Ishitsuka, Y. Recent Changes to Arctic River Discharge. *Nat. Commun.* **2021**, *12*, 6917. [CrossRef] [PubMed]
- Frederick, J.; Mota, A.; Tezaur, I.; Bull, D. A Thermo-Mechanical Terrestrial Model of Arctic Coastal Erosion. *J. Comput. Appl. Math.* **2021**, *397*, 113533. [CrossRef]
- Lisitzin, A.P. *Oceanic Sedimentation: Lithology and Geochemistry*; American Geophysical Union: Washington, DC, USA, 2013.
- Nielsen, D.M.; Pieper, P.; Barkhordarian, A.; Overduin, P.; Ilyina, T.; Brovkin, V.; Baehr, J.; Dobrynin, M. Increase in Arctic Coastal Erosion and Its Sensitivity to Warming in the Twenty-First Century. *Nat. Clim. Chang.* **2022**, *12*, 263–270. [CrossRef]
- Reimnitz, E.; Dethleff, D.; Nürnberg, D. Contrasts in Arctic Shelf Sea-Ice Regimes and Some Implications: Beaufort Sea versus Laptev Sea. *Mar. Geol.* **1994**, *119*, 215–225. [CrossRef]

15. Timmermans, M.-L.; Marshall, J. Understanding Arctic Ocean Circulation: A Review of Ocean Dynamics in a Changing Climate. *J. Geophys. Res. Oceans* **2020**, *125*, e2018JC014378. [[CrossRef](#)]
16. Eicken, H.; Reimnitz, E.; Alexandrov, V.; Martin, T.; Kassens, H.; Viehoff, T. Sea-Ice Processes in the Laptev Sea and Their Importance for Sediment Export. *Cont. Shelf Res.* **1997**, *17*, 205–233. [[CrossRef](#)]
17. Polyak, L.; Alley, R.B.; Andrews, J.T.; Brigham-Grette, J.; Cronin, T.M.; Darby, D.A.; Dyke, A.S.; Fitzpatrick, J.J.; Funder, S.; Holland, M.; et al. History of Sea Ice in the Arctic. *Quat. Sci. Rev.* **2010**, *29*, 1757–1778. [[CrossRef](#)]
18. Wegner, C.; Wittbrodt, K.; Hölemann, J.A.; Janout, M.A.; Krumpfen, T.; Selyuzhenok, V.; Novikhin, A.; Polyakova, Y.; Krykova, I.; Kassens, H.; et al. Sediment Entrainment into Sea Ice and Transport in the Transpolar Drift: A Case Study from the Laptev Sea in Winter 2011/2012. *Cont. Shelf Res.* **2017**, *141*, 1–10. [[CrossRef](#)]
19. Henderson, P. General Geochemical Properties and Abundances of the Rare Earth Elements. *Rare Earth Elem. Geochem.* **1984**, *2*, 1–32. [[CrossRef](#)]
20. Sholkovitz, E.R. The Aquatic Chemistry of Rare Earth Elements in Rivers and Estuaries. *Aquat. Geochem.* **1995**, *1*, 1–34. [[CrossRef](#)]
21. Tyler, G. Rare Earth Elements in Soil and Plant Systems—A Review. *Plant Soil* **2004**, *267*, 191–206. [[CrossRef](#)]
22. Chakhmouradian, A.R.; Wall, F. Rare Earth Elements: Minerals, Mines, Magnets (and More). *Elements* **2012**, *8*, 333–340. [[CrossRef](#)]
23. McLennan, S.M.; Ross Taylor, S. Geology, Geochemistry and Natural Abundances. In *Encyclopedia of Inorganic and Bioinorganic Chemistry*; John Wiley & Sons, Ltd.: Hoboken, NJ, USA, 2012; ISBN 9781119951438.
24. Fleet, A.J. Aqueous and Sedimentary Geochemistry of the Rare Earth Elements. *Dev. Geochem.* **1984**, *2*, 343–373. [[CrossRef](#)]
25. Astakhov, A.S.; Sattarova, V.V.; Xuefa, S.; Limin, H.; Aksentov, K.I.; Alatorsev, A.V.; Kolesnik, O.N.; Mariash, A.A. Distribution and Sources of Rare Earth Elements in Sediments of the Chukchi and East Siberian Seas. *Polar Sci.* **2019**, *20*, 148–159. [[CrossRef](#)]
26. Fangjian, X.U.; Anchun, L.I.; Tiegang, L.I.; Kehui, X.U.; Shiyue, C. Rare Earth Element Geochemistry in the Inner Shelf of the East China Sea and Its Implication to Sediment Provenances. *J. Rare Earths* **2011**, *29*, 702–709. [[CrossRef](#)]
27. Jung, H.; Lim, D.; Choi, J.; Yoo, H.; Rho, K.; Lee, H. Rare Earth Element Compositions of Core Sediments from the Shelf of the South Sea, Korea: Their Controls and Origins. *Cont. Shelf Res.* **2012**, *48*, 75–86. [[CrossRef](#)]
28. Liu, H.; Guo, H.; Pourret, O.; Wang, Z.; Sun, Z.; Zhang, W.; Liu, M. Distribution of Rare Earth Elements in Sediments of the North China Plain: A Probe of Sedimentation Process. *Appl. Geochem.* **2021**, *134*, 105089. [[CrossRef](#)]
29. Yang, S.Y.; Jung, H.S.; Choi, M.S.; Li, C.X. The Rare Earth Element Compositions of the Changjiang (Yangtze) and Huanghe (Yellow) River Sediments. *Earth Planet. Sci. Lett.* **2002**, *201*, 407–419. [[CrossRef](#)]
30. Zhang, X.; Zhang, F.; Chen, X.; Zhang, W.; Deng, H. REEs Fractionation and Sedimentary Implication in Surface Sediments from Eastern South China Sea. *J. Rare Earths* **2012**, *30*, 614–620. [[CrossRef](#)]
31. McLennan, S.M. Chapter 7. Rare Earth Elements in Sedimentary Rocks: Influence of Provenance and Sedimentary Processes. In *Geochemistry and Mineralogy of Rare Earth Elements*; Lipin, B.R., McKay, G.A., Eds.; De Gruyter: Berlin, Germany; Boston, MA, USA, 1989; pp. 169–200, ISBN 9781501509032.
32. Lee, S.-G.; Kim, J.-K.; Yang, D.-Y.; Kim, J.-Y. Rare Earth Element Geochemistry and Nd Isotope Composition of Stream Sediments, South Han River Drainage Basin, Korea. *Quat. Int.* **2008**, *176–177*, 121–134. [[CrossRef](#)]
33. Xu, Z.; Lim, D.; Choi, J. Rare Earth Elements in Bottom Sediments of Major Rivers around the Yellow Sea: Implications for Sediment Provenance. *Geo-Marine Lett.* **2009**, *29*, 291–300. [[CrossRef](#)]
34. Lim, D.; Jung, H.S.; Choi, J.Y. REE Partitioning in Riverine Sediments around the Yellow Sea and Its Importance in Shelf Sediment Provenance. *Mar. Geol.* **2014**, *357*, 12–24. [[CrossRef](#)]
35. Hu, S.; Zeng, Z.; Fang, X.; Zhu, B.; Li, X.; Chen, Z. Rare Earth Element Geochemistry of Sediments from the Southern Okinawa Trough since 3 Ka: Implications for River-Sea Processes and Sediment Source. *Open Geosci.* **2019**, *11*, 929–947. [[CrossRef](#)]
36. Ferhaou, S.; Kechiched, R.; Bruguier, O.; Sinisi, R.; Kocsis, L.; Mongelli, G.; Bosch, D.; Ameer-Zaimeche, O.; Laouar, R. Rare Earth Elements plus Yttrium (REY) in Phosphorites from the Tébessa Region (Eastern Algeria): Abundance, Geochemical Distribution through Grain Size Fractions, and Economic Significance. *J. Geochem. Explor.* **2022**, *241*, 107058. [[CrossRef](#)]
37. Rachold, V. Major, Trace and Rare Earth Element Geochemistry of Suspended Particulate Material of East Siberian Rivers Draining to the Arctic Ocean. In *Land-Ocean Systems in the Siberian Arctic: Dynamics and History*; Springer: Berlin/Heidelberg, Germany, 1999; pp. 199–222. [[CrossRef](#)]
38. Laukert, G.; Frank, M.; Bauch, D.; Hathorne, E.C.; Gutjahr, M.; Janout, M.; Hölemann, J. Transport and Transformation of Riverine Neodymium Isotope and Rare Earth Element Signatures in High Latitude Estuaries: A Case Study from the Laptev Sea. *Earth Planet. Sci. Lett.* **2017**, *477*, 205–217. [[CrossRef](#)]
39. Sattarova, V.; Astakhov, A.; Aksentov, K.; Shi, X.; Hu, L.; Liu, Y.; Polyakov, D.; Alatorsev, A.; Kolesnik, O. Geochemistry of the Laptev and East Siberian Seas Sediments with Emphasis on Rare-Earth Elements: Application for Sediment Sources and Paleooceanography. *Cont. Shelf Res.* **2023**, *254*, 104907. [[CrossRef](#)]
40. Baranov, B.; Galkin, S.; Vedenin, A.; Dozorova, K.; Gebruk, A.; Flint, M. Methane Seeps on the Outer Shelf of the Laptev Sea: Characteristic Features, Structural Control, and Benthic Fauna. *Geo-Marine Lett.* **2020**, *40*, 541–557. [[CrossRef](#)]
41. Macdonald, R.W.; Kuzyk, Z.A.; Johannessen, S.C. It Is Not Just about the Ice: A Geochemical Perspective on the Changing Arctic Ocean. *J. Environ. Stud. Sci.* **2015**, *5*, 288–301. [[CrossRef](#)]
42. Blott, S.J.; Pye, K. GRADISTAT: A Grain Size Distribution and Statistics Package for the Analysis of Unconsolidated Sediments. *Earth Surf. Process. Landf.* **2001**, *26*, 1237–1248. [[CrossRef](#)]

43. Folk, R.L. The Distinction between Grain Size and Mineral Composition in Sedimentary-Rock Nomenclature. *J. Geol.* **1954**, *62*, 344–359. [[CrossRef](#)]
44. Shepard Francis, P. Nomenclature Based on Sand-Silt-Clay Ratios. *SEPM J. Sediment. Res.* **1954**, *24*, 151–158. [[CrossRef](#)]
45. Gromet, L.P.; Haskin, L.A.; Korotev, R.L.; Dymek, R.F. The “North American Shale Composite”: Its Compilation, Major and Trace Element Characteristics. *Geochim. Cosmochim. Acta* **1984**, *48*, 2469–2482. [[CrossRef](#)]
46. Astakhov, A.S.; Semiletov, I.P.; Sattarova, V.V.; Shi, X.; Hu, L.; Aksentov, K.I.; Vasilenko, Y.P.; Ivanov, M.V. Rare Earth Elements in the Bottom Sediments of the East Arctic Seas of Russia as Indicators of Terrigenous Input. *Dokl. Earth Sci.* **2018**, *482*, 1324–1327. [[CrossRef](#)]
47. Chaillou, G.; Anschutz, P.; Lavaux, G.; Blanc, G. Rare Earth Elements in the Modern Sediments of the Bay of Biscay (France). *Mar. Chem.* **2006**, *100*, 39–52. [[CrossRef](#)]
48. Wang, S.; Zhang, N.; Chen, H.; Li, L.; Yan, W. The Surface Sediment Types and Their Rare Earth Element Characteristics from the Continental Shelf of the Northern South China Sea. *Cont. Shelf Res.* **2014**, *88*, 185–202. [[CrossRef](#)]
49. Gordeev, V.V.; Sidorov, I.S. Concentrations of Major Elements and Their Outflow into the Laptev Sea by the Lena River. *Mar. Chem.* **1993**, *43*, 33–45. [[CrossRef](#)]
50. Osadchiv, A.; Medvedev, I.; Shchuka, S.; Kulikov, M.; Spivak, E.; Pisareva, M.; Semiletov, I. Influence of Estuarine Tidal Mixing on Structure and Spatial Scales of Large River Plumes. *Ocean Sci.* **2020**, *16*, 781–798. [[CrossRef](#)]
51. Pavlov, V.; Timokhov, L.; Baskakov, G.; Kulakov, M. *Hydrometeorological Regime of the Kara, Laptev, and East-Siberian Seas*; Applied Physics Laboratory, University of Washington: Washington, DC, USA, 1994.
52. Alabyan, A.M.; Chalov, R.S.; Korotaev, V.N.; Sidorchuk, A.Y.; Zaitsev, A.A. Natural and Technogenic Water and Sediment Supply to the Laptev Sea. *Rep. Polar Res.* **1995**, *176*, 265–271.
53. Dudarev, O.V.; Charkin, A.N.; Shakhova, N.E.; Mazurov, A.K.; Semiletov, I.P. *Modern Lithomorphogenesis in the East Arctic Russian Shelf*; Tomsk Polytechnic University: Tomsk, Russia, 2016; ISBN 978-5-4387-0737-0.
54. Rachold, V.; Grigoriev, M.N.; Are, F.E.; Solomon, S.; Reimnitz, E.; Kassens, H.; Antonow, M. Coastal Erosion vs Riverine Sediment Discharge in the Arctic Shelf Seas. *Int. J. Earth Sci.* **2000**, *89*, 450–460. [[CrossRef](#)]
55. Brüchert, V.; Bröder, L.; Sawicka, J.E.; Tesi, T.; Joye, S.P.; Sun, X.; Semiletov, I.P.; Samarkin, V.A. Carbon Mineralization in Laptev and East Siberian Sea Shelf and Slope Sediment. *Biogeosciences* **2018**, *15*, 471–490. [[CrossRef](#)]
56. Taylor, S.R.; McLennan, S.M. Chapter 79 The Significance of the Rare Earths in Geochemistry and Cosmochemistry. In *Two-Hundred-Year Impact of Rare Earths on Science*; Handbook on the Physics and Chemistry of Rare Earths; Elsevier: Amsterdam, The Netherlands, 1988; Volume 11, pp. 485–578.
57. Grigoriev, M.N.; Kunitsky, V.V.; Chzhan, R.V.; Shepelev, V.V. On the Variation in Geocryological, Landscape and Hydrological Conditions in the Arctic Zone of East Siberia in Connection with Climate Warming. *Geogr. Nat. Resour.* **2009**, *30*, 101–106. [[CrossRef](#)]
58. *Atlas Arktiki*; AANII and GUGK: Moscow, Russia, 1985. (In Russian)
59. Charette, M.A.; Kipp, L.E.; Jensen, L.T.; Dabrowski, J.S.; Whitmore, L.M.; Fitzsimmons, J.N.; Williford, T.; Ulfsbo, A.; Jones, E.; Bundy, R.M.; et al. The Transpolar Drift as a Source of Riverine and Shelf-Derived Trace Elements to the Central Arctic Ocean. *J. Geophys. Res. Oceans* **2020**, *125*, e2019JC015920. [[CrossRef](#)]
60. Gordienko, P.A.; Laktionov, A.F. Circulation and Physics of the Arctic Basin Waters. In *Oceanography*; Annals of The International Geophysical Year; Gordon, A.L., Baker, F.W.G., Eds.; Pergamon Press: Oxford, UK, 1969; Volume 46, pp. 94–112, ISBN 978-1-4832-1306-4.
61. Mysak, L.A. Patterns of Arctic Circulation. *Science* **2001**, *293*, 1269–1270. [[CrossRef](#)] [[PubMed](#)]
62. Kechiched, R.; Laouar, R.; Bruguier, O.; Kocsis, L.; Salmi-Laouar, S.; Bosch, D.; Ameer-Zaimeche, O.; Foufou, A.; Larit, H. Comprehensive REE + Y and Sensitive Redox Trace Elements of Algerian Phosphorites (Tébessa, Eastern Algeria): A Geochemical Study and Depositional Environments Tracking. *J. Geochem. Explor.* **2020**, *208*, 106396. [[CrossRef](#)]
63. Bau, M. Controls on the Fractionation of Isovalent Trace Elements in Magmatic and Aqueous Systems: Evidence from Y/Ho, Zr/Hf, and Lanthanide Tetrad Effect. *Contrib. Mineral. Petrol.* **1996**, *123*, 323–333. [[CrossRef](#)]
64. Huang, J.; Wan, S.; Xiong, Z.; Zhao, D.; Liu, X.; Li, A.; Li, T. Geochemical Records of Taiwan-Sourced Sediments in the South China Sea Linked to Holocene Climate Changes. *Palaeogeogr. Palaeoclimatol. Palaeoecol.* **2016**, *441*, 871–881. [[CrossRef](#)]
65. Prego, R.; Caetano, M.; Bernárdez, P.; Brito, P.; Ospina-Alvarez, N.; Vale, C. Rare Earth Elements in Coastal Sediments of the Northern Galician Shelf: Influence of Geological Features. *Cont. Shelf Res.* **2012**, *35*, 75–85. [[CrossRef](#)]
66. Taylor, S.R.; McLennan, S.M. *The Continental Crust: Its Composition and Evolution*; Blackwell: Boston, MA, USA, 1985.
67. Li, M.; Ouyang, T.; Zhu, Z.; Tian, C.; Peng, S.; Tang, Z.; Qiu, Y.; Zhong, H.; Peng, X. Rare Earth Element Fractionations of the Northwestern South China Sea Sediments, and Their Implications for East Asian Monsoon Reconstruction during the Last 36 Kyr. *Quat. Int.* **2019**, *525*, 16–24. [[CrossRef](#)]
68. Mao, L.; Mo, D.; Yang, J.; Guo, Y.; Lv, H. Rare Earth Elements Geochemistry in Surface Floodplain Sediments from the Xiangjiang River, Middle Reach of Changjiang River, China. *Quat. Int.* **2014**, *336*, 80–88. [[CrossRef](#)]
69. Li, L.; Liu, Y.; Wang, X.; Hu, L.; Yang, G.; Wang, H.; Bosin, A.A.; Astakhov, A.S.; Shi, X. Early Diagenesis and Accumulation of Redox-Sensitive Elements in East Siberian Arctic Shelves. *Mar. Geol.* **2020**, *429*, 106309. [[CrossRef](#)]
70. Bau, M.; Dulski, P. Distribution of Yttrium and Rare-Earth Elements in the Penge and Kuruman Iron-Formations, Transvaal Supergroup, South Africa. *Precambrian Res.* **1996**, *79*, 37–55. [[CrossRef](#)]

71. Och, L.M.; Müller, B.; Wichser, A.; Ulrich, A.; Vologina, E.G.; Sturm, M. Rare Earth Elements in the Sediments of Lake Baikal. *Chem. Geol.* **2014**, *376*, 61–75. [[CrossRef](#)]
72. Lina, S.S.; Fernandes, L.L.; Rao, V.P. Distribution and Fractionation of Rare Earth Elements and Yttrium in Suspended and Bottom Sediments of the Kali Estuary, Western India. *Environ. Earth Sci.* **2017**, *76*, 174. [[CrossRef](#)]
73. Möller, P.; Dulski, P.; Luck, J. Determination of Rare Earth Elements in Seawater by Inductively Coupled Plasma-Mass Spectrometry. *Spectrochim. Acta Part B At. Spectrosc.* **1992**, *47*, 1379–1387. [[CrossRef](#)]

**Disclaimer/Publisher’s Note:** The statements, opinions and data contained in all publications are solely those of the individual author(s) and contributor(s) and not of MDPI and/or the editor(s). MDPI and/or the editor(s) disclaim responsibility for any injury to people or property resulting from any ideas, methods, instructions or products referred to in the content.